

## Electrical impedance spectrum transformation of liver tissues under the influence of temperature

T. Pryimak, O. Popadynets, I. Gasiuk, T. Kotyk

*Vasyl Stefanyk Precarpathian National University*

*Department of Materials Science and New Technology, 57 T. Shevchenko St., Ivano-Frankivsk, 76025, Ukraine*

In this article the analysis of the electric impedance spectra of liver samples was performed. Nyquist diagrams were built for intact and experimental samples that were exposed to temperature. The optimal model equivalent electrical circuits of the studied systems are obtained and processed, an attempt to establish the correspondence of individual elements of equivalent circuits and their real analogues in the studied tissues was made and the parameters of component circuits are calculated. It is shown that the initial stages of thermotemporal transformation of the tissue structure are reflected in the change of the parameters of the elements of the schemes and the final irreversible destructive effects are manifested in the form of loss of their elements. In addition, structural deformations of tissues were examined by optical microscopy. The conclusion about features of influence of temperature on the investigated samples and on the general structure of equivalent electric schemes was made.

**KEYWORDS:** equivalent circuit, constant phase element, electrical impedance, destructive influence, liver.

Date of Submission: 16-11-2021

Date of Acceptance: 01-12-2021

### I. INTRODUCTION

The need to study the features of processes, factors of destruction and damage of biological tissues is due to the importance of preserving their structural integrity for use in industries where these factors play an important role. One of the most studied factors of influence is temperature and its negative values are actively used in medicine.

The influence of cryosurgical methods causes "thermal stress", which occurs when there is a drastic change in the freezing process to heating process [1, 2]. In addition, such values are usually used for storage and freezing of meat, which is important in the field of food technology [3, 4].

Due to the fact that it is not always possible to maintain a stable low or high temperature, for example, during transportation, its abrupt changes can lead to a number of freeze-thaw cycles. The result is a violation of metabolism, structure of proteins and lipids [5, 6].

In addition, an additional cause of damage at low temperatures is the formation of ice in the outer cell space and dehydration of cells at high concentrations [7, 8].

It should be noted that the use of cryosurgical methods can contribute to the process of death, or necrosis, the signs of which must be recognized in the early stages for the preservation and subsequent use of organs [9].

Necrosis is characterized by specific manifestations, in particular, the development of inflammation in the affected areas, chromatin condensation and destruction of membrane structures [10, 11].

Necrosis is preceded by the process of necrobiosis, the early stages of which are called oncosis [12]. It is characterized by changes in the shape and volume of the cell that occur within a few minutes from the beginning of the action of aggressive factor. Its signs can be recognized by checking the capacity of the cell to propidium iodide or trypan blue.

Necrosis is actively studied, for example, in the case of acute and chronic liver disease and depending on the degree and size of the affected area, there are several types, including spotted, zonal and partial [13].

Microscopic analysis of the affected cells can detect a number of signs of this process, in particular the appearance of cytosolic and membrane vesicles in the vascular space with their gradual exfoliation [14].

To prevent and monitor the occurrence of destruction processes, specific methods of biomaterial research are used, in particular, the method of pulsed photothermal radiometry, which, for example, is used to assess the impact of laser surgery [15].

In cryotherapy there are methods that allow to visualize the results of treatment: vibroacoustography [16], ultrasound monitoring [17] and electrical impedance tomography (EIT) [18].

One of the most well-known and promising non-destructive methods of control is electrical impedance spectroscopy (IC) [19], which allows to characterize the structural features of tissues based on their passive electrical properties and is the basis of EIT.

Impedance measurement involves the passage of alternating current through the object of study at a certain frequency which allows to obtain information about changes in volume to classify tissues based on their conductive and dielectric properties [20].

The essence of the method is to measure the frequency ( $\omega$ ) dependence of the real ( $Z'$ ) and imaginary part ( $Z''$ ) of the complex electrical impedance of the object to obtain a parametric frequency ( $\omega$ ) dependence:  $Z'(\omega) = f(Z''(\omega))$  (Nyquist diagrams) and interpretation of the results obtained by constructing an electrical equivalent circuit and calculating the parameters of its components by various mathematical and software tools [21].

At present, experiments have been conducted using bioimpedance to assess the overall impact of low temperatures, thawing and freezing processes [22, 23], thermal damage [24, 25, 26] to study the characteristics of changes of impedance in tissue over time [27]. In the field of food technology, IP has been used to determine the freshness of meat when stored in ice [28]. Attempts have also been made to detect early signs of necrotic processes using cryosurgical methods [29].

Given that electrical equivalent models are not often used to measure the degree of damage of the studied material, the aim of the study was to show the results of changes of impedance in organ tissue under the influence of positive temperatures by creating appropriate equivalent schemes, explaining changes in their parameters and comparing results with optical microscopy.

## II. MATERIALS AND METHODS

The use of separate tissues for the experiment allowed to control the size of the samples according to the size of the cells used and contributed to more accurate measurement due to the uniformity of the temperature influence.

It was decided to select the pig liver as the object of measurement due to the availability of the material and the relative prevalence of its use. The samples obtained immediately after slaughter and were stored in a thermostat at a certain temperature.

The test cells were made of a 2 ml plastic syringe body. The ends of the cylindrical sample were in contact with the nickel mesh. Nickel conductors welded to the mesh served as a current collector. The structure of the experimental equivalent scheme is chosen similar to that given by us in the previous work [30].

Cylindrical samples, 1.2 cm high, weighing 1 - 1.5 g and 2 cm in diameter, were placed in a sealed thermostat 1/120 SPU under the influence of temperatures of 2 °C, 8 °C, 12 °C, 25 °C and 35 °C for 2, 8 and 14 hours.

Impedance spectroscopy was performed using an AUTOLAB PGStat 30 spectrometer in the frequency range 0.01 Hz - 100 kHz. To reduce the influence of the amplitude values of the voltage of the measuring signal on the state of organic tissues the potential range was set to 0 - 5 mV.

Numerical processing of measurement results to determine the parameters of the elements of equivalent circuits was performed using software environments FRA-2, Origin and Z-View 2, respectively.

In order to demonstrate the effects of temperature exposure at the tissue and cell levels optical microscopy of experimental samples was performed in which the structure of equivalent models differed from the corresponding intact models.

For histological examination tissue samples were fixed in a 10% solution of neutral formalin which was replaced every 12 and 24 hours. After 14 days the material was transferred to paraffin blocks on a sled microtome where sections with a thickness of 5  $\mu$ m were made followed then by staining with hematoxylin and eosin according to conventional methods. Trichrome Mason and Hart staining were used to identify collagen and elastic fibers, respectively.

The obtained histological sections were examined using a Micros Austria MC300 light microscope and a Sony TouPCam 5.1M UHCCD digital camera with a TouPTek Photonics AMA075 TouPView v.3 adapter.

## III. RESULTS AND DISCUSSION

The experimentally obtained Nyquist diagrams of the studied samples for different temperatures stored for 2, 8 and 14 hours are shown in Figures 2, 6 and 11. The frequency range of the obtained spectra is 0.01 Hz - 100 kHz.  $Z'$  and  $-Z''$  are the real and imaginary components of the impedance, respectively. The tabs show the high-frequency parts of the spectra, the arrows indicate the directions of frequency increase.

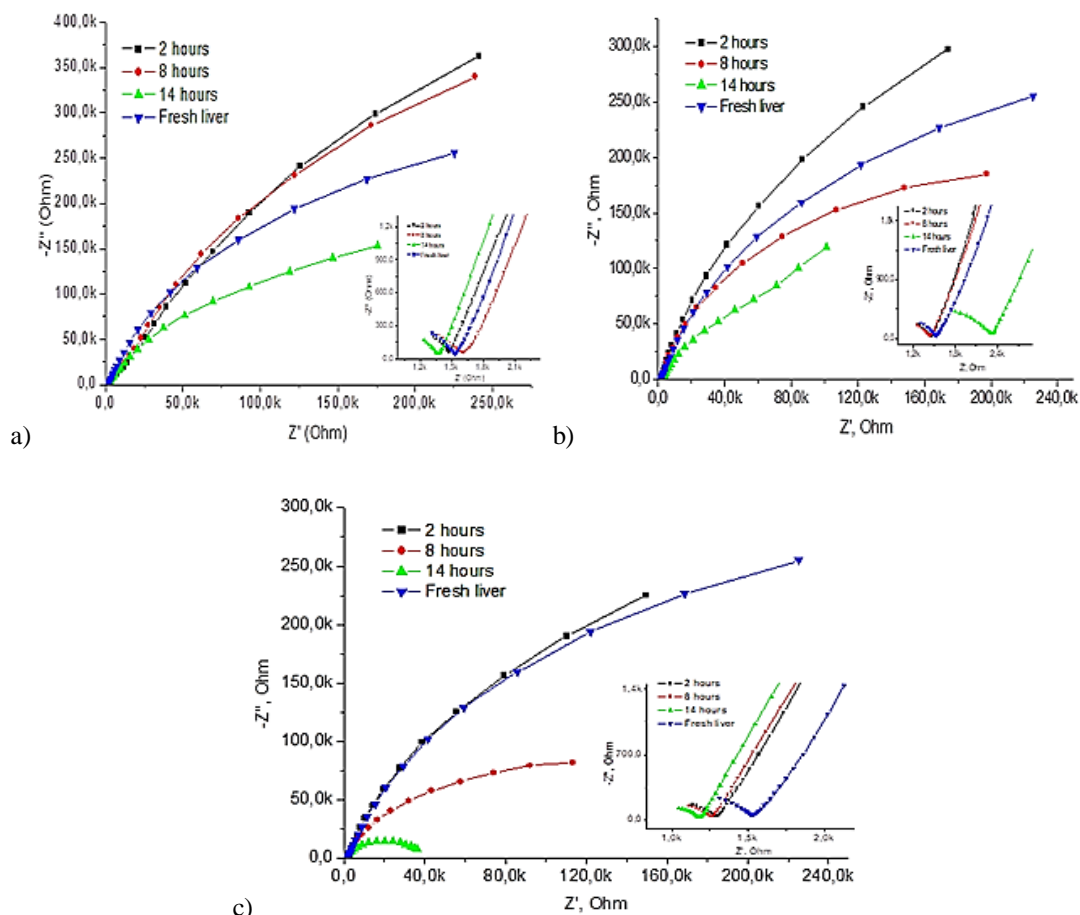


Fig. 1. impedance spectra of liver tissues stored at a) 2 ° C, b) 8 ° C, and c) 12 ° C.

Analysis of the above diagrams of Nyquist (Fig. 1) allowed to build the corresponding electrical equivalent circuits.

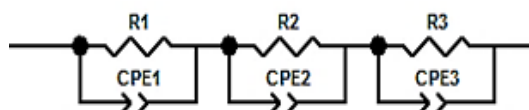


Fig. 2. electrical equivalent circuit of liver samples: intact sample, sample at 2 ° C, 8 ° C and 12 ° C for 2, 8 and 14 hours.

The values of the parameters of the components of these schemes are given in table 1. For comparison, all the following tables show the values of the parameters of the scheme of the intact sample. CPE and R- parameters of electrical equivalent circuits of samples under the influence of

2, 8 and 12 ° C, where R is the resistance and CPE-T is the constant phase element for which the intermediate elements between the active resistance are determined (at CPE-P = 0) or an ideal capacitor (CPE-P = 1). For CPE-P < 1, the element is defined as a pseudocapacitor.

Table. 1. Parameters of equivalent schemes (Fig. 2).

Degrees	Time, hours	CPE1-T, F	CPE1-P	R1, Ohm	CPE2-T, F	CPE2-P	R2, Ohm	CPE3-T, F	CPE3-P	R3, Ohm
2	2	$2,6 \cdot 10^{-5}$	$9,2 \cdot 10^{-1}$	$9,4 \cdot 10^2$	$3,7 \cdot 10^{-5}$	$7,1 \cdot 10^{-1}$	$2,2 \cdot 10^4$	$1,5 \cdot 10^{-8}$	$6,8 \cdot 10^{-1}$	$1,5 \cdot 10^3$
	8	$2,7 \cdot 10^{-5}$	$9,3 \cdot 10^{-1}$	$8,9 \cdot 10^2$	$3,9 \cdot 10^{-5}$	$7,1 \cdot 10^{-1}$	$2,5 \cdot 10^4$	$2,8 \cdot 10^{-7}$	$4,7 \cdot 10^{-1}$	$1,7 \cdot 10^3$
	14	$7,2 \cdot 10^{-4}$	1,3	$7,4 \cdot 10^3$	$2,6 \cdot 10^{-5}$	$7,7 \cdot 10^{-1}$	$4,3 \cdot 10^3$	$3,8 \cdot 10^{-8}$	$6,1 \cdot 10^{-1}$	$1,4 \cdot 10^3$
8	2	$2,8 \cdot 10^{-5}$	$8,8 \cdot 10^{-1}$	$9,9 \cdot 10^2$	$1,4 \cdot 10^{-4}$	$7,2 \cdot 10^{-1}$	$3,4 \cdot 10^2$	$5,1 \cdot 10^{-8}$	$6 \cdot 10^{-1}$	$1,5 \cdot 10^3$
	8	$3 \cdot 10^{-5}$	$9 \cdot 10^{-1}$	$4,3 \cdot 10^3$	$1,3 \cdot 10^{-4}$	$6,9 \cdot 10^{-1}$	$6,1 \cdot 10^2$	$5,3 \cdot 10^{-8}$	$6 \cdot 10^{-1}$	$1,5 \cdot 10^3$
	14	$3,7 \cdot 10^{-5}$	$1,8 \cdot 10^{-5}$	$6,6 \cdot 10^2$	$3,7 \cdot 10^{-5}$	$7,6 \cdot 10^{-1}$	$3,6 \cdot 10^3$	$7,4 \cdot 10^{-8}$	$6,3 \cdot 10^{-1}$	$1,7 \cdot 10^3$
12	2	$3,3 \cdot 10^{-5}$	$8,7 \cdot 10^{-1}$	$7 \cdot 10^2$	$1,3 \cdot 10^{-4}$	$7,2 \cdot 10^{-1}$	$1,1 \cdot 10^3$	$7,5 \cdot 10^{-8}$	$5,7 \cdot 10^{-1}$	$1,3 \cdot 10^3$
	8	$4,1 \cdot 10^{-5}$	$8,3 \cdot 10^{-1}$	$2 \cdot 10^3$	$1,7 \cdot 10^{-4}$	$8,4 \cdot 10^{-1}$	$2,6 \cdot 10^2$	$1 \cdot 10^{-7}$	$5,5 \cdot 10^{-1}$	$1,3 \cdot 10^3$
	14	$1,2 \cdot 10^{-4}$	$7,2 \cdot 10^{-1}$	$2,4 \cdot 10^4$	$7,7 \cdot 10^{-8}$	$5,7 \cdot 10^{-1}$	$1,2 \cdot 10^3$	$1 \cdot 10^{-4}$	$9,9 \cdot 10^{-1}$	$1,6 \cdot 10^4$
Intact sample		$2,4 \cdot 10^{-5}$	$8,6 \cdot 10^{-1}$	$6,7 \cdot 10^2$	$1,4 \cdot 10^{-4}$	$6,1 \cdot 10^{-1}$	$6,3 \cdot 10^2$	$3 \cdot 10^{-8}$	$6,4 \cdot 10^{-1}$	$1,5 \cdot 10^3$

The dynamics of changes in the parameters of the schemes (Table 1a) allows us to draw conclusions about the feasibility and effectiveness of the chosen method for a similar characteristic of the electrical properties of tissues. When storing the sample at 2 ° C, there are no significant differences in the values of the capacity of intact and experimental samples which is due to the expected low destructive effect of the selected temperature.

Minor, monotonic changes in the parameter can potentially be explained by passive changes in the electrolyte composition near the bilipid layer. In the case of CPE-P which conditionally reflects the permeability of the membrane a slight decrease in

the parameter over time is observed in the case of CPE1-P and CPE2-P. However, the value of CPE1-P at 14 hours, indicates the incorrectness of the corresponding equivalent scheme. The R-parameter also does not show either a significant difference in values between groups of samples, except for R2, and a clear dynamics of changes over time.

A similar situation is observed at 8 ° C and 12 ° C. A slight decrease in capacity is observed in CPE3-T and, in part, in CPE1-T parameters. In the case of permeability and resistance, no significant differences between the experimental samples from the values of intact or changes over time are observed, both at 8 ° C and at 12 ° C.

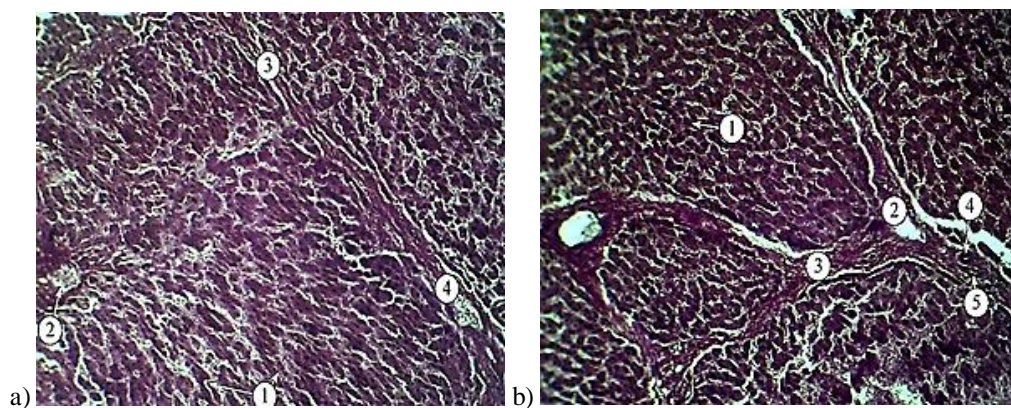


Fig. 3. intact sample: a) 1 - hepatic plates, 2 - central vein, 3 - layers of loose connective tissue, 4 - blood vessels; sample at 8 ° C: b) 1 - hepatic plates, 2 - interparticle vein, 3 - layers of loose connective tissue, 4 - interparticle artery, 5 - interparticle bile duct. Coloring: according to Hart. Coll. : x100.

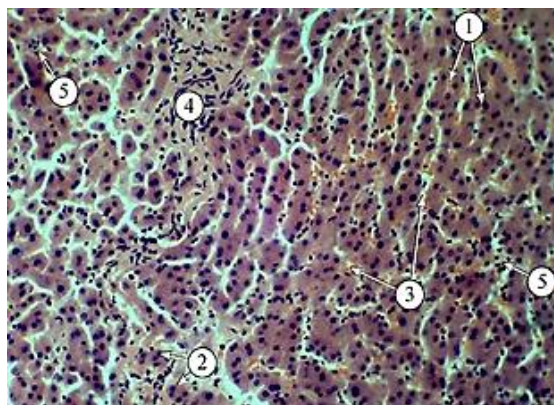


Fig. 4. sample at 8 °C: 1 - hepatic plates, 2 - dinuclear hepatocytes, 3 - sinusoid, 4 - layers of loose connective tissue, 5 - lympho-histiocytic infiltrates. Staining: hematoxylin and eosin. Coll.: x200.

In light-optical examination in all fields of view there is a clear separation of particles due to well-developed interparticle connective tissue (Fig. 3 - 4) which identifies collagen and elastic fibers.

At the apex of the hepatic lobules, in the portal spaces, there are triads which include the interparticle arteries, veins and bile ducts. Arranged, arranged in rows, hepatocytes - hepatic plates which are radially directed to the central vein - are

visualized in lobes. Due to this specificity of architecture in the hepatic lobe, the central, intermediate and peripheral zones are distinguished.

In the middle of a hepatic plate biliary tubules are visible, between plates there are sinusoids. Hepatocytes are polygonal in shape, often have two nuclei (Fig. 4). In general, there are no clear signs of any significant damage.

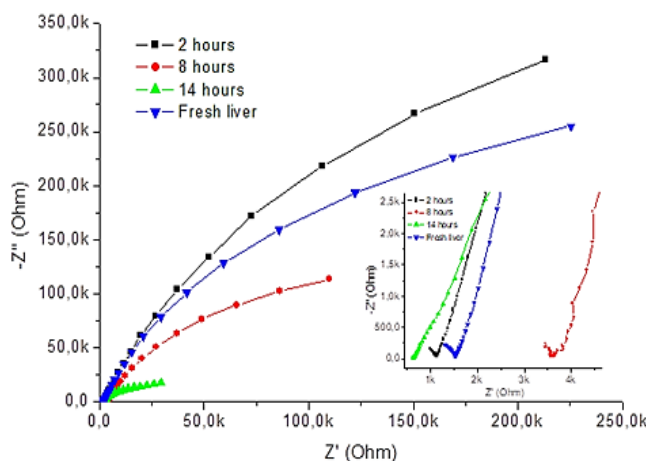


Fig. 5. transformation of the impedance spectra of liver tissues at a temperature of 25 °C.

The structure of the developed electrical equivalent circuit is identical to the circuit shown in Fig. 2.

Tab. 2. CPE and R-parameters of electrical equivalent circuits of samples under the influence of 25 °C.

Degrees	Time, hours	CPE1-T, F	CPE1-P	R1, Ohm	CPE2-T, F	CPE2-P	R2, Ohm	CPE3-T, F	CPE3-P	R3, Ohm
25	2	$2,5 \cdot 10^{-5}$	$8,7 \cdot 10^{-1}$	$1 \cdot 10^6$	$1,3 \cdot 10^{-4}$	$6,1 \cdot 10^{-1}$	$2,4 \cdot 10^3$	$4,8 \cdot 10^{-8}$	$6,2 \cdot 10^{-1}$	$1,1 \cdot 10^3$
	8	$4,5 \cdot 10^{-5}$	$8,3 \cdot 10^{-1}$	$3,2 \cdot 10^5$	$5,3 \cdot 10^{-5}$	$6,8 \cdot 10^{-1}$	$2,9 \cdot 10^2$	$6 \cdot 10^{-9}$	$6,2 \cdot 10^{-1}$	$3,6 \cdot 10^3$
	14	$1,4 \cdot 10^{-4}$	$5,8 \cdot 10^{-1}$	$9 \cdot 10^4$	$2,9 \cdot 10^{-4}$	$9,8 \cdot 10^{-1}$	$7,1 \cdot 10^3$	$1,9 \cdot 10^{-10}$	$9,4 \cdot 10^{-1}$	$6,3 \cdot 10^2$
Intact sample		$2,4 \cdot 10^{-5}$	$8,6 \cdot 10^{-1}$	$6,7 \cdot 10^5$	$1,35 \cdot 10^{-4}$	$6,1 \cdot 10^{-1}$	$6,3 \cdot 10^2$	$3 \cdot 10^{-8}$	$6,4 \cdot 10^{-1}$	$1,5 \cdot 10^3$

The effect of 25 °C shows a significantly different parameter of CPE1-T experimental and intact samples and a slight decrease in CPE2-P, CPE3-P and R1, R3 parameters over time, respectively.

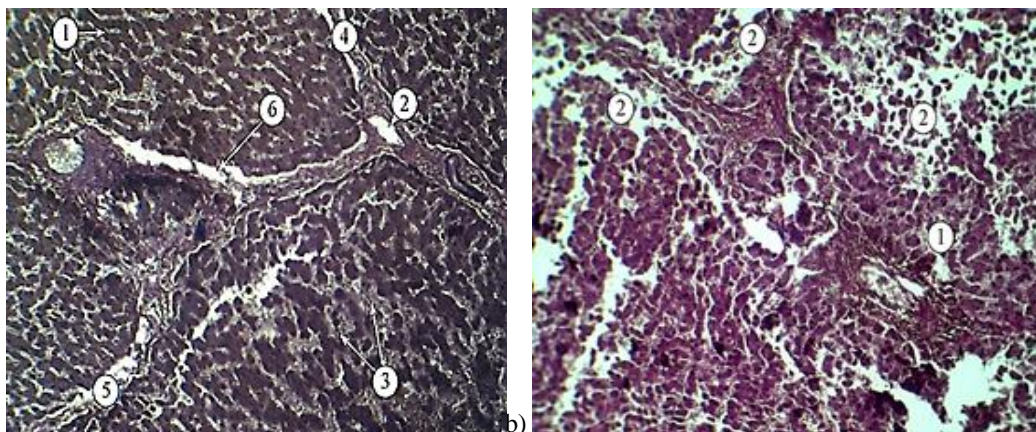


Fig. 6.a) 1 - hepatic plates, 2 - interlobular vein, 3 - dilated sinusoids, 4 - compacted layers of loose connective tissue, 5 - damaged areas of interparticle connective tissue layers, 6 - peripheral edema; b) 1 - disorganized liver plates, 2 - destruction of the peripheral zone of the lobe. Coloring: according to Hart. Coll. : x100.

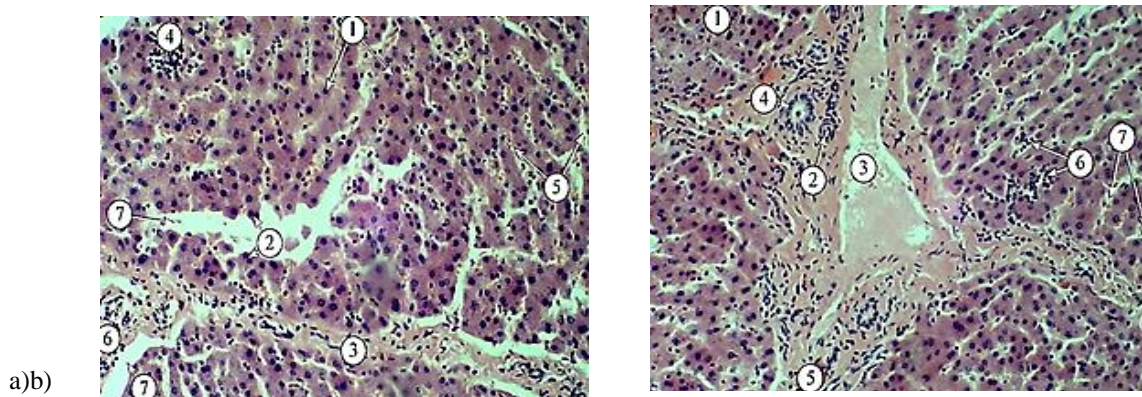


Fig. 7.a) 1 - hepatic plates, 2 - two nuclear hepatocytes, 3 - layers of loose connective tissue, 4 - lympho-plasmacytic infiltrates, 5 - sinusoids, 6 - interparticle bile duct, 7 - edema of the peripheral zone of the lobe; b) 1 - hepatic plates, 2 - interparticle artery, 3 - interparticle vein with stasis, 4 - interparticle bile duct, 5 - layers of loose connective tissue, 6 - lympho-plasmacytic infiltrates, 7 - sinusoids. Staining: hematoxylin and eosin. Coll. : x200.

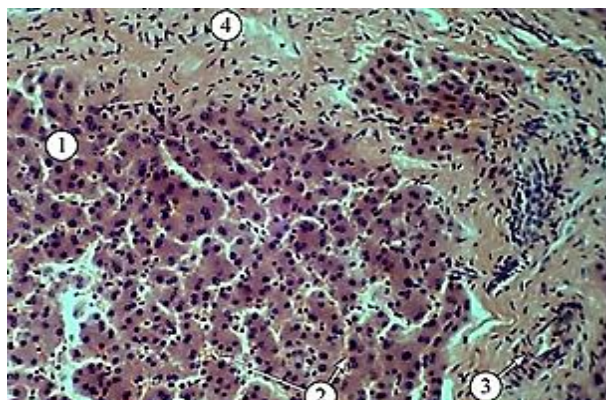


Fig. 8.1 - hepatic plates, 2 - sinusoids, 3 - interparticle artery, 4 - fluffy, swollen areas of interparticle connective tissue layers. Staining: hematoxylin and eosin. Coll. : x200.

The results of microscopy of the corresponding samples show the preserved lobular

principle of structure, however, structural changes are revealed both in the connective tissue skeleton and in the parenchymal component (Figs. 6 - 8).

In some areas there are visible seals of interparticle connective tissue (Fig. 8), as well as edema, fibrosis and local destruction. Blood stasis, dilation and plethora of sinusoids are observed in the interparticle veins (Fig. 6b).

Violations of intercellular contacts are found in peripheral zones, as a result, there is a noticeable disorganization of hepatic plates (Fig. 6). The contours of hepatocytes are blurred, lympho-plasmacytic infiltrates are common (Fig. 7b).

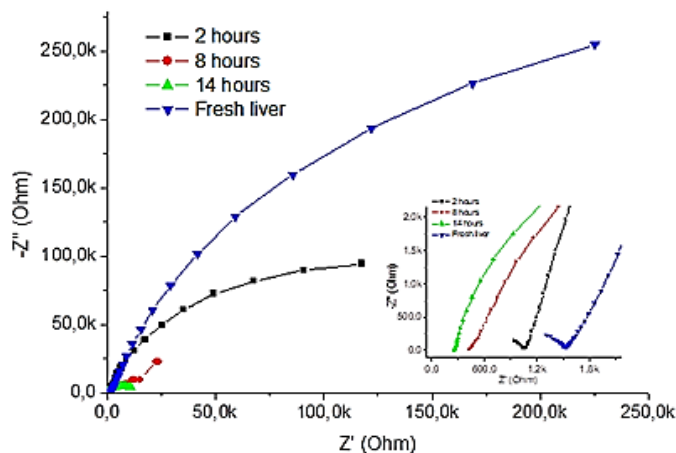


Fig. 9. impedance spectra of liver tissues at a temperature of 35 ° C.

Analysis of Nyquist diagrams (Fig. 9) for a storage temperature of 35 ° C allowed to build the corresponding electrical equivalent circuits (Fig. 10).

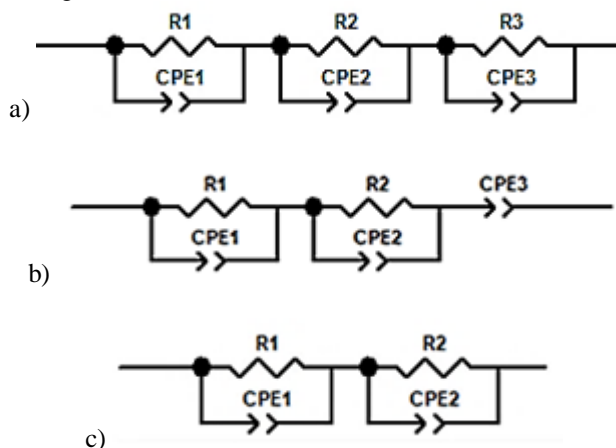


Fig. 10. electrical equivalent circuits of liver samples for spectra of samples at a temperature of 35 ° C for a) - 2, b) - 8 and c) - 14 hours.

Significant thermal tissue damage which has been shown to occur at temperatures close to 37 ° C and above is visually reflected by the formation of

edema and blisters, increased intercellular space and general disorganization of liver plates according to the results of optical microscopy described below.

Tab. 3. Parameters of electrical equivalent circuits of samples under the influence of 35 ° C.

Degrees	Time, hours	CPE1-T, F	CPE1-P	R1, Ohm	CPE2-T, F	CPE2-P	R2, Ohm	CPE3-T, F	CPE3-P	R3, Ohm
35	2	$7,3 \cdot 10^{-5}$	$9,3 \cdot 10^{-1}$	$2,6 \cdot 10^1$	$3 \cdot 10^{-8}$	$6,6 \cdot 10^{-1}$	$1,1 \cdot 10^3$	$4,6 \cdot 10^{-5}$	$8,7 \cdot 10^{-1}$	$2,3 \cdot 10^5$
	8	$3 \cdot 10^{-8}$	$5,5 \cdot 10^{-1}$	$4,3 \cdot 10^2$	$1,8 \cdot 10^{-4}$	$9,8 \cdot 10^{-1}$	$4,7 \cdot 10^3$	$2,4 \cdot 10^{-4}$	$6,4 \cdot 10^{-1}$	-
	14	$2,3 \cdot 10^{-7}$	$4 \cdot 10^{-1}$	$2,5 \cdot 10^2$	$2,7 \cdot 10^{-4}$	$8,6 \cdot 10^{-1}$	$1,2 \cdot 10^4$	-	-	-
Intactsample		$2,4 \cdot 10^{-5}$	$8,6 \cdot 10^{-1}$	$6,7 \cdot 10^5$	$1,35 \cdot 10^{-4}$	$6,1 \cdot 10^{-1}$	$6,3 \cdot 10^2$	$3 \cdot 10^{-5}$	$6,4 \cdot 10^{-1}$	$1,5 \cdot 10^5$

At the cellular level such processes are accompanied by destruction of the cytoskeleton and, as a consequence, the plasma membrane [31, 32]. As a result, the amount of free electrolytes increases due to the leakage of intracellular ions into the extracellular space and the volume of extracellular fluid which can potentially cause a decrease in the values of capacitive elements of experimental samples, in particular at 35 ° C (Table 3), increasing the conductivity and correspondingly decreasing the modulus of impedance that correlates with the temperature value. [33, 34]

In addition, the decrease in capacity may be due to a decrease in the permeability of the plasma membrane and, as a consequence, the number of mobile ions. This could potentially be accompanied by an increase in the CPE-P parameter observed in the CPE-P1 values. One of the reasons for the decrease in the permeability of the membrane may be its complete structural destruction under the influence of temperature which is probably reflected in the absence of both CPE-P3 and capacity.

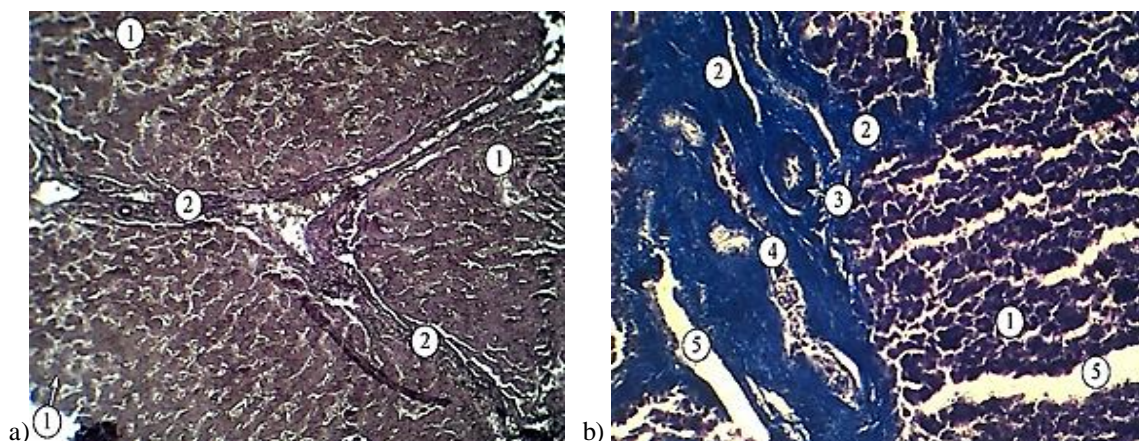


Fig. 11. a) 1 - disorganized liver plates, 2 - compacted areas of interparticle connective tissue layers; b) 1 - disorganized liver plates, 2 - compacted areas of interparticle connective tissue layers, 3 - interparticle artery, 4 - interparticle vein, 5 - edema. Color: trichrome according to Mason. Coll.: x100.

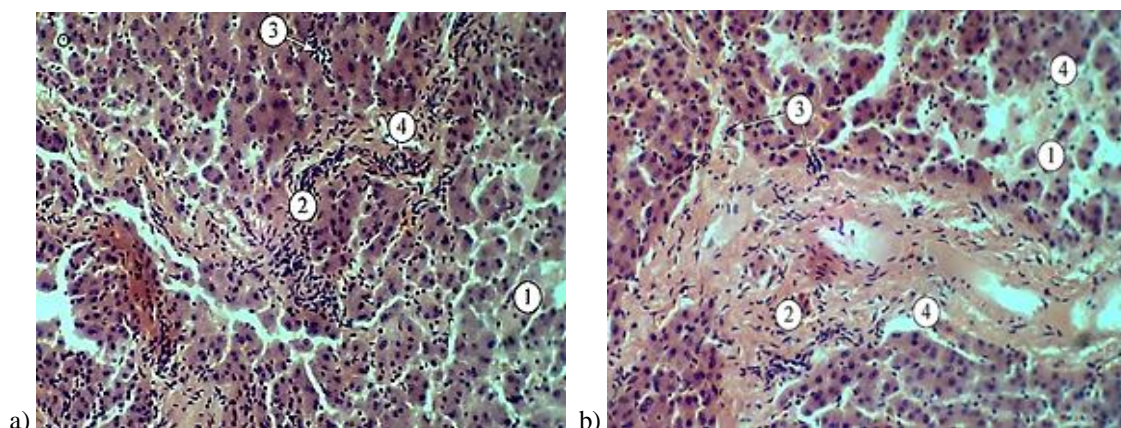


Fig. 12. a) 1 - disorganized hepatic plates, 2 - compacted areas of interparticle connective tissue layers, 3 - lympho-plasmacytic infiltrates, 4 - interparticle bile duct; b) 1 - disorganized liver plates, 2 - compacted areas of interparticle connective tissue layers, 3 - lympho-plasmacytic infiltrates, 4 - edema. Staining: hematoxylin and eosin. Coll.: x200.

The results of microscopy of the corresponding samples show more pronounced edematous-dystrophic changes and disorganization of the liver plates than in previous cases (Fig. 11 - 12).

There are noticeable seals and deformations in the stroma, elastic fibers are thinned (Fig. 11a) and there are noticeable loci with swollen collagen fibers and edematous changes in the portal spaces and in the wall of the components of the liver triad (Fig. 11b).

It is worth noting the stasis in the sinusoids of the intermediate zone of the lobe (Fig. 13a) and the loss of radial architecture (Fig. 11, 12). Weak eosinophilia of the cytoplasm of hepatocytes and lympho-plasmacytic infiltration are also observed (Fig. 12).

#### IV. CONCLUSIONS

The gradual increase in temperature and time of its influence contributes to the destruction of tissues due to the caused necrosis which is manifested by the corresponding changes in the structure of the equivalent electrical circuit of the studied samples. The critical value at which such processes occur among the studied temperatures are temperatures close to 35 ° C. Potential causes are membrane destruction and mixing of extracellular and intracellular contents which is reflected in the disappearance of the relevant components of the model, in particular CPE3 and R3.

Temporal changes of thermostabilized samples are manifested primarily by changes in the parameters of the circuits of the impedance sample, in the future, for higher temperatures, the transformation of a directly equivalent circuit.

Thus, the analysis of experimental spectra of electrical impedance can serve as a sufficiently informative tool for expressive analysis of the degree of destruction of liver tissues.

#### REFERENCES

- [1]. Yu, T., Liu, J., & Zhou, Y. EVIDENCES OF THERMAL STRESS WAVE INDUCED IN DEEPLY FROZEN BIOMATERIALS BY A STRONG AND INSTANTANEOUS HEATING. *Journal of Thermal Stresses*, 27, 2004, 1089 - 1100.
- [2]. Purschke M, Laubach HJ, Anderson RR, Manstein D. Thermal injury causes DNA damage and lethality in unheated surrounding cells: active thermal bystander effect. *J Invest Dermatol*. 2010 Jan;130(1):86-92. DOI: 10.1038/jid.2009.205.
- [3]. Wazir H, Chay SY, Zarei M, et al. Effects of Storage Time and Temperature on Lipid Oxidation and Protein Co-Oxidation of Low-Moisture Shredded Meat Products. *Antioxidants (Basel)*. 2019;8(10):486. Published 2019 Oct 16. DOI:10.3390/antiox8100486.
- [4]. Soyer Ayla, Özalp Berna, Dalmış Ülkü, Bilgin Volkan. Effects of freezing temperature and duration of frozen storage on lipid and protein oxidation in chicken meat *Food Chemistry*. 2010 Jun;120(4):1025-1030. DOI: 10.1016/j.foodchem.2009.11.042.
- [5]. Ji X, Wang M, Li L, Chen F, Zhang Y, Li Q, Zhou J. The Impact of Repeated Freeze-Thaw Cycles on the Quality of Biomolecules in Four Different Tissues. *Biopreserv Biobank*. 2017 Oct;15(5):475-483. DOI: 10.1089/bio.2017.0064.
- [6]. Guntur SR, Lee KI, Paeng DG, Coleman AJ, Choi MJ. Temperature-dependent thermal properties of ex vivo liver undergoing thermal ablation. *Ultrasound Med Biol*. 2013 Oct;39(10):1771-84. DOI: 10.1016/j.ultrasmedbio.2013.04.014. Epub 2013 Aug 9.
- [7]. Han B, Bischof JC. Direct cell injury associated with eutectic crystallization during freezing. *Cryobiology*. 2004;48(1):8-21. DOI:10.1016/j.cryobiol.2003.11.002
- [8]. Gage AA. Correlation of electrical impedance and temperature in tissue during freezing. *Cryobiology*. 1979;16(1):56-62. DOI:10.1016/0011-2240(79)90010-5.
- [9]. Gage AA, Baust J. Mechanisms of tissue injury in cryosurgery. *Cryobiology*. 1998; 37(3):171-186. DOI: 10.1006/cryo.1998.2115.
- [10]. Biochemical mechanisms of apoptosis: a textbook / LI Ostapchenko, TV Sinelnik, TV Rybalchenko, VK Rybalchenko. - Kyiv: Publishing and Printing Center "Kyiv University", 2018. - 310 p. - ISBN 978-966-439-302-4: B.c.
- [11]. Golstein P, Kroemer G. Cell death by necrosis: towards a molecular definition. *Trends Biochem Sci*. 2007;32(1):37-43. DOI: 10.1016/j.tibs.2006.11.001.
- [12]. P, Buja LM. Oncosis: an important non-apoptotic mode of cell death. *Exp Mol Pathol*. 2012;93(3):302-308. DOI:10.1016/j.yexmp.2012.09.018.
- [13]. Krishna, M. (2017), Patterns of necrosis in liver disease. *Clinical Liver Disease*, 10: 53-56. DOI:10.1002/cld.653.
- [14]. Trump BF, Berezsky IK, Chang SH, Phelps PC. The pathways of cell death: oncosis, apoptosis, and necrosis. *Toxicol Pathol*. 1997;25(1):82-88. DOI: 10.1177/019262339702500116.

- [15]. Chebotareva, Galina & Zubov, Boris & Nikitin, Alexander & Nikiforov, Sergey & Chebotarev, Andrey. (1996). Pulsed photothermal radiometry of surgical laser-tissue interaction. *Proc SPIE*. 5-16. DOI:10.1117/12.239566.
- [16]. Mitri FG, Davis BJ, Alizad A, et al. Prostate cryotherapy monitoring using vibroacoustography: preliminary results of an ex vivo study and technical feasibility. *IEEE Trans Biomed Eng*. 2008;55(11):2584-2592. DOI:10.1109/TBME.2008.2001284.
- [17]. Rhame, Ellen E et al. "Ultrasonographic guidance and characterization of cryoanalgesic lesions in treating a case of refractory sural neuroma." *Case reports in anesthesiology* vol. 2011 (2011): 691478. DOI:10.1155/2011/691478
- [18]. Edd JF, Ivorra A, Horowitz L, Rubinsky B. Imaging cryosurgery with EIT: tracking the ice front and post-thaw tissue viability. *Physiol Meas*. 2008 Aug;29(8):899-912. DOI: 10.1088/0967-3334/29/8/004.
- [19]. Grossi, Marco & Riccò, Bruno. (2017). Electrical impedance spectroscopy (EIS) for biological analysis and food characterization: A review. *Journal of Sensors and Sensor Systems*. 6. 303-325. DOI: 10.5194/jsss-6-303-2017.
- [20]. Stahn, Alexander & Terblanche, Elmarie & Gunga, Hanns-Christian. (2012). Use of Bioelectrical Impedance: General Principles and Overview. DOI: 10.1007/978-1-441 9-1788-1\_3.
- [21]. Dean DA, Ramanathan T, Machado D, Sundararajan R. Electrical Impedance Spectroscopy Study of Biological Tissues. *J Electrostat*. 2008;66(3-4):165-177. DOI:10.1016/j.elstat.2007.11.005
- [22]. Stout DG. Effect of cold acclimation on bulk tissue electrical impedance: I. Measurements with birdsfoot trefoil at subfreezing temperatures. *Plant Physiol*. 1988;86(1):275-282. DOI:10.1104/pp.86.1.275.
- [23]. Fischer, G et al. "Impedance and conductivity of bovine myocardium during freezing and thawing at slow rates - implications for cardiac cryo-ablation." *Medical engineering & physics* vol. 74 (2019): 89-98. DOI:10.1016/j.medengphy.2019.09.017
- [24]. Yu TH, Liu J, Zhou YX. Using electrical impedance detection to evaluate the viability of biomaterials subject to freezing or thermal injury. *Anal Bioanal Chem*. 2004;378(7):1793-1800. DOI: 10.1007/s00216-004-2508-2.
- [25]. Kobayashi, A., Mizutani, K., Wakasaki, N., & Maeda, Y. (2013). Changes of electrical impedance characteristic of pork in heating process. *International Proceedings of Chemical, Biological & Environmental Engineering*, 5074-78. DOI: 10.7763/ipcbee.2013.v50.16.
- [26]. Schmidt FC, Fuentes A, Masot R, Alcañiz M, Laurindo JB, Barat JM. Assessing heat treatment of chicken breast cuts by impedance spectroscopy. *Food Sci Technol Int*. 2017 Mar;23(2):110-118. DOI: 10.1177/1082013216659609.
- [27]. M. Guermazi, O. Kanoun and N. Derbel, "Investigation of Long Time Beef and Veal Meat Behavior by Bioimpedance Spectroscopy for Meat Monitoring," in *IEEE Sensors Journal*, vol. 14, no. 10, pp. 3624-3630, Oct. 2014, DOI: 10.1109/JSEN.2014.2328858.
- [28]. Fan, X., Lin, X., Wu, C., Zhang, N., Cheng, Q., Qi, H., Konno, K., & Dong, X. (2020). Estimating freshness of ice storage rainbow trout using bioelectrical impedance analysis. *Food science & nutrition*, 9(1), 154-163. DOI:https://doi.org/10.1002/fsn3.1974.
- [29]. Gage, A.A et al. "Tissue impedance and temperature measurements in relation to necrosis in experimental cryosurgery." *Cryobiology* vol.22,3 (1985): 282-8. DOI:10.1016/0011-2240(85)90148-8
- [30]. Pryimak TV TRANSFORMATION OF THE SPECTRUM OF ELECTRIC IMPEDANCE OF BIOLOGICAL TISSUES UNDER THE INFLUENCE OF DESTRUCTIVE FACTORS [Electronic resource] / TV Pryimak, IM Gasyuk, AB Grubyak Lutsk, №71, 2021. DOI: https://doi.org/10.36910/6775.24153966.2021.71.18.
- [31]. 31.M.W. Miller, M.C. Ziskin, Biological consequences of hyperthermia, *Ultrasound Med. Biol*. 15 (1989) 707-722.
- [32]. Coss, R A, and W A Linnemans. "The effects of hyperthermia on the cytoskeleton: a review." *International journal of hyperthermia : the official journal of European Society for Hyperthermic Oncology, North American Hyperthermia Group* vol. 12,2 (1996): 173-96. DOI:10.3109/02656739609022507.
- [33]. Wei, Ran et al. "Effect of freezing on electrical properties and quality of thawed chicken breast meat." *Asian-Australasian journal of animal sciences* vol. 30,4 (2017): 569-575. DOI:10.5713/ajas.16.0435

- [34]. Huang, Yu-Jie et al. "The correlation between extracellular resistance by electrical biopsy and the ratio of optical low staining area in irradiated intestinal tissues of rats." *Biomedical engineering online* vol. 12,23. 19 Mar. 2013, DOI:10.1186/1475-925X-12-23

T. Pryimak, et. al. "Electrical impedance spectrum transformation of liver tissues under the influence of temperature." *International Journal of Engineering Research and Applications (IJERA)*, vol.11 (12), 2021, pp 01-11.